International Research Journal of Engineering and Technology (IRJET) e-ISSN: 2395-0056
Volume: 06 Issue: 03 | Mar 2019 www.irjet.net p-ISSN: 2395-0072

Thermomagnetic-gravitational convection in a vertical layer of ferrofluid in an applied magnetic field

Mst. Lovly Khatun[1], Md. Habibur Rahman[2],

[1]Department of Mathematics, Khulna University of Engineering & Technology
Khulna-9203, Bangladesh
[2]Associate Professor, Department of Mathematics,
Khulna University of Engineering & Technology
Khulna-9203, Bangladesh

Abstract– *Linear stability of thermomagnetic-gravitational convection in a layer of ferrofluid between two vertical differentially heated non-magnetic plates in a uniform oblique external magnetic field has been investigated. For each set of physical governing parameters, the equivalent problem is solved for a range of wave numbers. The arising thermomagnetic convection is occurred by the spatial variation of magnetization happening due to its dependence on the temperature. In particular, the variation of fluid magnetisation due to thermal disturbances is found to have a destabilizing effect. In this article, both gravitational and magnetic effects acting simultaneously are accounted for. The characteristics of all instability modes are investigated, and three main types of instability patterns corresponding to thermo-gravitational, magnetic and magneto-gravitational convection are observed to exist in a normal magnetic field. However, the oblique external magnetic field leads to the preferential shift of instability structures toward the hot wall, which introduces a further asymmetry and a qualitative change in the stability characteristics compared to the normal field case. It is noticed that for each field inclination angle there exists a preferred field orientation angle that promotes the onset of magneto-gravitational instability the most.*

Key Words: ferrofluids, convection, magnetic field, temperature, instability.

1. INTRODUCTION

This is the property of cobalt, nickel, iron, their alloys and some minerals that have these metals as compounds. Magnetic properties of such materials weaken as their temperature increases, and they are lost completely above a certain temperature called Curie point. Curie point is below the melting temperature of ferromagnetics so that the melts of ferromagnetic materials are non-magnetic. In contrast to melts, magnetic fluids are multi-phase media containing solid magnetic particles that can be magnetized. Such suspensions can be used to transfer heat, and heat and mass transport in such liquid magnetic can be controlled by using an external magnetic field. Synthetic magnetic fluids, also known as ferrofluids, are electrically non-conducting stable colloidal suspensions consisting of the carrier liquid (kerosene, water or mineral oil) and magnetic (iron, cobalt, nickel etc.) nanoparticles with the characteristic size $d_p \approx 10$ nm covered by surfactants (oleic acid) to prevent them

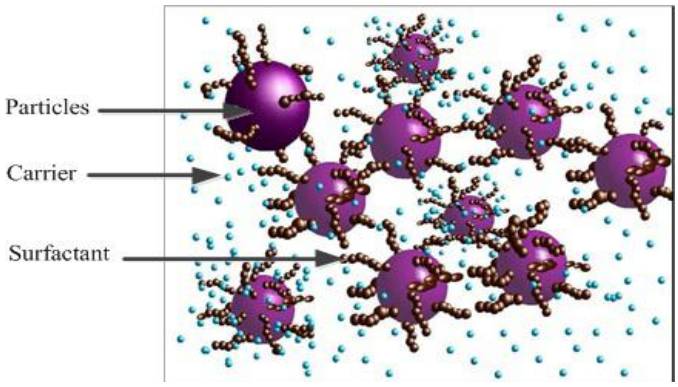

Figure 1: Formation of surfacted ferrofluid.

from forming aggregates. The most widely studied ferrofluids contain colloidal magnetite (Fe_3O_4). A typical ferromagnetic fluid can have up to 10% of magnetic solids and up to 10% of surfactant by volume [1]. Due to the demagnetization and the chemical adsorption impact at the boundary of the magnetic core, there is a layer of demagnetized magnetite of thickness ~1

nm near the particle boundary. As seen from Figure 1 each particle is coated with an appropriate surfactant and the resulting fluid is known as surfacted ferrofluid. Consistent with the previous studies [2, 3] a planar geometry is considered as a fluid layer is confined by long and wide non-magnetic plates. The choice of such a classical geometry is dictated by a number of factors. Firstly, it is a common prototype configuration for realistic heat exchangers. Secondly, it allows one to make a significant analytical and computational progress without being overwhelmed by geometrical details. Thirdly, this geometry is relatively easy to realize in experiments. The results for thermo-gravitational and mixed magneto-gravitational convection in a layer of ferrofluid in a uniform normal and oblique external magnetic field have been investigated rather than our previous study of pure thermomagnetic convection in the gravity-free environment [4]. The comprehensive discussion about the problem for different values of representative parameters is reported in Rahman and Suslov [5]. In this paper, the selected representative numerical results and values of the determined critical parameters and the physical nature of instabilities characterized by them are presented.

2. PROBLEM FORMULATION

Consider a layer of a ferromagnetic fluid that fills a gap between two infinitely long and wide parallel non-magnetic plates shown in figure 2. The plates are separated by the distance $2d$ and are maintained at constant different temperatures $T_* \pm \Theta$. An external uniform magnetic field, $\vec{H} = (H_x^e, H_y^e, H_z^e)$ such that $\left|\vec{H}^e\right| = H^e$ where $H_x^e = H^e \cos\delta$, $H_y^e = H^e \sin\delta\cos\gamma$ and $H_z^e = H^e \sin\delta\sin\gamma$, is applied at an arbitrary inclination to the layer. This field causes an internal magnetic field $\vec{H}$ such that $\left|\vec{H}\right| = H$ within the layer. The external field induces fluid magnetization $\vec{M}$ such that $\left|\vec{M}\right| = M$, which is assumed to be co-directed with the internal magnetic field: $\vec{M} = \chi_* \vec{H}_*$, where χ_* is the integral magnetic susceptibility of the fluid. Here $\chi = \partial\vec{M}/\partial\vec{H}$ is the differential magnetic susceptibility defined at reference location. The gravity vector $\vec{g}$ has constant components $(0, -\vec{g}, 0)$ acting in the opposite direction of y axis is vertical and parallel to the plates.

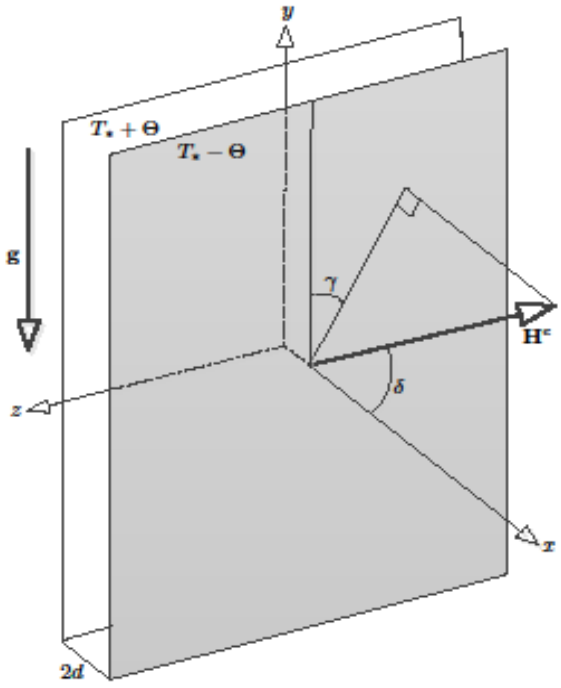

Figure 2: Experimental model of the problem. The external applied magnetic field, $\vec{H}^e$ makes arbitrary angles δ and γ with the coordinate axes.

The governing equations of the problem are

$$\nabla.\vec{v} = 0, \tag{1}$$

$$\rho_* \frac{\partial \vec{v}}{\partial t} + \rho_* \vec{v}.\nabla\vec{v} = -\nabla P + \eta_* \nabla^2 \vec{v} + \rho\vec{g} + \mu_0 M\, \nabla H, \tag{2}$$

$$\frac{\partial T}{\partial t} + \vec{v}.\nabla T = \kappa_* \nabla^2 T, \tag{3}$$

$$\nabla \times \vec{H} = 0, \nabla.\vec{B} = 0, \tag{4}$$

where

$$\vec{B} = \mu_0(\vec{M} + \vec{H}), \vec{M} = \frac{M(H,T)}{H}\vec{H}. \tag{5}$$

In the above equations $\vec{v}$ is the velocity vector with the respective components (u, v, w) in the x, y and z directions, t is time, T is the temperature, P is the pressure, B is the magnetic induction, ρ_* is the fluid density, η_* is the dynamic viscosity, κ_* is the thermal diffusivity of the fluid, and $\mu_0 = 4\pi \times 10^{-7}$ H/m is the magnetic constant. The subscript $*$ denotes the values of the fluid properties evaluated at the reference temperature T_* and reference internal magnetic field H_*

3. NON-DIMENSIONAL GOVERNING EQUATIONS

Non-dimensional governing equations are

$$\nabla.\vec{v} = 0, \tag{6}$$

$$\frac{\partial \vec{v}}{\partial t} + \vec{v}.\nabla\vec{v} = -\nabla P + \nabla^2\vec{v} - Gr\theta\vec{e}_g - Gr_m\theta\nabla H, \tag{7}$$

$$\frac{\partial \theta}{\partial t} + \vec{v}.\nabla\theta = \frac{1}{\Pr}\nabla^2\theta, \tag{8}$$

$$\nabla \times \vec{H} = 0, \tag{9}$$

$$(1+\chi_*)\nabla.\vec{H} + (\chi - \chi_*)\nabla H.\vec{e}_* - (1+\chi_*)\nabla\theta.\vec{e}_* = 0, \tag{10}$$

$$\vec{M} = [(\chi - \chi_*)(H - N) - (1+\chi)\theta]\vec{e}_* + \lambda_*\vec{H}, \tag{11}$$

where $\vec{e}_g = (0,-1,0)$ and $\vec{e}_* = \vec{H}_*/H_*$ with the boundary conditions~

$$[\vec{H}^e - \{(\chi - \chi_*)(H - N) \pm (1+\chi_*)\}\vec{e}_* - (1+\chi_*)\vec{H}].\vec{\eta} = 0, \tag{12}$$

$$\vec{v} = 0, \theta = \mp 1 \text{ at } x = \pm 1. \tag{13}$$

The dimensionless parameters appearing in the problem are

$$Gr = \frac{\rho_*^2 \beta_* \Theta g d^3}{\eta_*^2}, Gr_m = \frac{\rho_* \mu_0 K^2 \Theta^2 d^2}{\eta_*^2(1+\chi)},$$
$$\Pr = \frac{\eta_*}{\rho_* \kappa_*}, \qquad N = \frac{H_*(1+\chi)}{K\Theta}. \tag{14}$$

where the thermal and magnetic Grashof numbers Gr and Gr_m characterize the importance of buoyancy and magnetic forces, respectively; Prandtl number Pr characterizes the ratio of viscous and thermal diffusion transports, and parameter N describes the strength of the magnetic field at the reference location in the system.

4. LINEARIZED PERTURBATION EQUATIONS

After Squire's transformation linearised perturbation equations (normal mode form~ $e^{\tilde{\sigma}t + i\tilde{\alpha}y}$) become

$$D\tilde{u} + i\tilde{\alpha}\tilde{v} = 0, \tag{15}$$

$$\tilde{\sigma}\tilde{u} + (\tilde{\alpha}^2 + i\tilde{\alpha}\tilde{v}_0 - D^2)\tilde{u} + D\tilde{P} + \tilde{e}_{10}\tilde{G}r_m D\tilde{H}_{x0}\tilde{\theta} + \tilde{G}r_m\tilde{\theta}_0\tilde{e}_{10}D^2\tilde{\phi}$$
$$+ \tilde{G}r_m\tilde{\theta}_0[i\tilde{\alpha}\tilde{e}_{20} + (1-\tilde{e}_{10}^2)\frac{D\tilde{H}_{x0}}{\tilde{H}_0}]D\tilde{\phi} - i\tilde{\alpha}\tilde{G}r_m\tilde{\theta}_0\tilde{e}_{10}\tilde{e}_{20}\frac{D\tilde{H}_{x0}}{\tilde{H}_0}\tilde{\phi} = 0, \tag{16}$$

$$\tilde{\sigma}\tilde{v} + D\tilde{v}_0\tilde{u} + (\tilde{\alpha}^2 + i\tilde{\alpha}\tilde{v}_0 - D^2)\tilde{v} + i\tilde{\alpha}\tilde{P} - \tilde{G}r\tilde{\theta}$$
$$+ \tilde{\alpha}\tilde{G}r_m\tilde{\theta}_0(i\tilde{e}_{10}D\tilde{\phi} - \tilde{\alpha}\tilde{e}_{20}\tilde{\phi}) = 0, \tag{17}$$

$$\tilde{\sigma}\tilde{\theta} + D\tilde{\theta}_0\tilde{u} + (\frac{\tilde{\alpha}^2 - D^2}{\tilde{\mathrm{Pr}}} + i\tilde{\alpha}\tilde{v}_0)\tilde{\theta} = 0, \tag{18}$$

$$(D^2 - \tilde{\alpha}^2)\tilde{\phi} - \frac{\tilde{\chi} - \tilde{\chi}_*}{1+\tilde{\chi}_*}\tilde{\alpha}\tilde{e}_{20}[\tilde{\alpha}\tilde{e}_{20*} + i\tilde{e}_{10*}\tilde{e}_{10}\frac{D\tilde{H}_{x0}}{\tilde{H}_0}]\tilde{\phi}$$
$$+ \frac{\tilde{\chi} - \tilde{\chi}_*}{1+\tilde{\chi}_*}[i\tilde{\alpha}(\tilde{e}_{10}\tilde{e}_{20*} + \tilde{e}_{10*}\tilde{e}_{20}) + \tilde{e}_{10*}(1-\tilde{e}_{10}^2)\frac{D\tilde{H}_{x0}}{\tilde{H}_0}]D\tilde{\phi} \tag{19}$$
$$+ \frac{\tilde{\chi} - \tilde{\chi}_*}{1+\tilde{\chi}_*}\tilde{e}_{10*}\tilde{e}_{10}D^2\tilde{\phi} - \frac{1+\tilde{\chi}}{1+\tilde{\chi}_*}[i\tilde{\alpha}\tilde{e}_{20*} + \tilde{e}_{10*}D]\tilde{\theta} = 0,$$

with the boundary conditions

$$(1+\tilde{\chi}_*)D\tilde{\phi} \pm |\tilde{\alpha}|\tilde{\phi} + \tilde{e}_{10*}(\tilde{\chi} - \tilde{\chi}_*)(i\tilde{\alpha}\tilde{e}_{20} + \tilde{e}_{10}D)\tilde{\phi} = 0 \tag{20}$$

$$\tilde{u} = \tilde{v} = \tilde{\theta} = 0 \text{ at } \tilde{x} = \pm 1. \tag{21}$$

where $D = d/dx$, and $\tilde{v}_0 = \tilde{G}r(\tilde{x}^3 - \tilde{x})/6$ and $\tilde{\theta}_o = -\tilde{x}$ are the basic flow velocity and temperature profiles. These above mentioned equations represent an equivalent two-dimensional problem form that enables one to reduce the computational cost of stability calculations. However, the external applied magnetic field still remains three-dimensional in the above Squire-transformed linearised equations and thus the two coordinate angles δ and γ still act as independent control parameters of the problem. The δ angle parameterizes the deviation of the field from the normal direction while γ measures the azimuthal angle from the direction of gravity.

5. REPRESENTATIVE STABILITY CHARACTERISTICS OF FLOWS IN NORMAL MAGNETIC FIELD

Three main types of convection patterns: thermo-gravitational, magnetic and mixed magneto-gravitational convection are found to exist. The corresponding typical eigen-value curves are shown in figures 3, 4 and 5, respectively. In the first case $(\tilde{G}r_m \to 0)$ one maximum of the disturbance amplification rate $\tilde{\sigma}^R$ exists with complex conjugate eigen-values (see figure 3) that indicate the existence of two counter-propagating waves. In the second case $(\tilde{G}r \to 0)$ one maximum of the disturbance amplification rate $\tilde{\sigma}^R$ is also found but now eigen-values are real (see figure 4). This situation corresponds to a stationary magneto-convection pattern. In the third case $(\tilde{G}r \neq 0, \tilde{G}r_m \neq 0)$ there are three maxima of the disturbance amplification rate $\tilde{\sigma}^R$ (see figure 5) of which the left-and right-most maxima correspond to thermo-gravitational convection while the middle one corresponds to a stationary magneto-convection pattern. Numerical values of the critical parameters for these three types of convection in a perpendicular field for various values of Prandtl number $\tilde{\mathrm{Pr}}$ are obtained by solving equations (15)–(21) and are given in Table 1. As follows from Table 1 the increase in Prandtl number leads to the increase of a wave number. As a result the distance between two instability rolls decreases. Note that the disturbance wave speed becomes larger than the maximum basic flow velocity in a large Prandtl-number fluid meaning that the physical nature of instabilities has nothing to do with the basic flow velocity field.

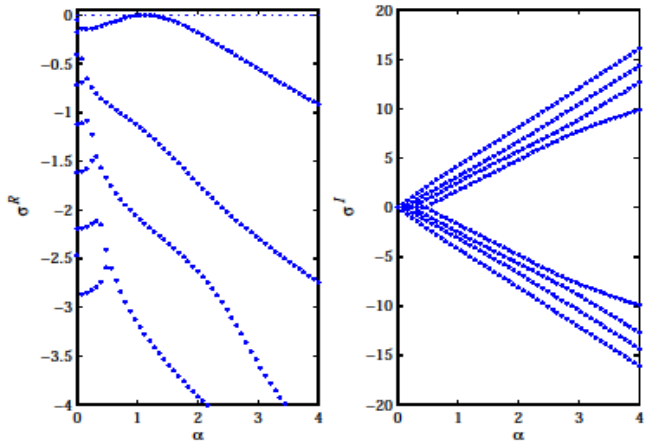

Figure 3: Leading disturbance temporal amplification rates $\tilde{\sigma}^R$ (left) and frequencies $\tilde{\sigma}^I$ (right) as functions of the combined wave number $\tilde{\sigma}$ for $(\tilde{Gr}_m, \tilde{Gr}) \equiv (0, 65.33)$ (onset of thermo-gravitational convection) at $\delta = \gamma = 0^o$ and $\chi = \chi_* = 5$.

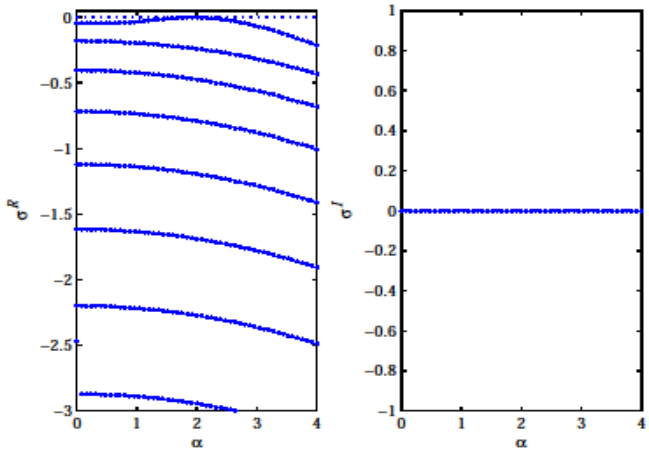

Figure 4: Same as Figure 3 but for $(\tilde{Gr}_m, \tilde{Gr}) \equiv (3.31, 0)$ (onset of stationary magneto convection).

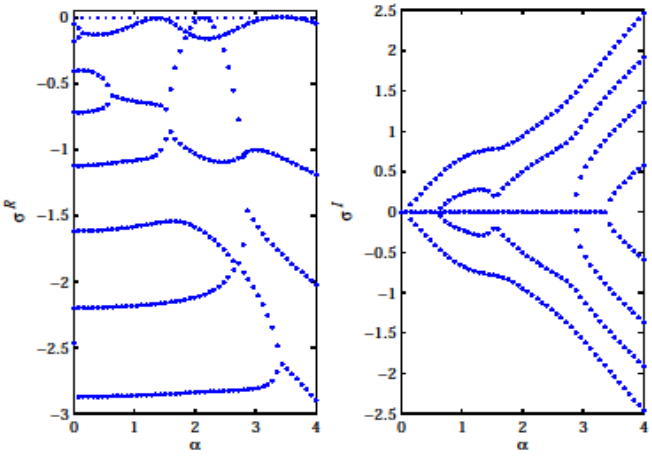

Figure 5: Same as Figure 3 but for $(\tilde{Gr}_m, \tilde{Gr}) \equiv (43.92, 12)$. In the left plot the left and right maxima correspond to small- and large-wave number thermomagnetic waves, respectively, and the middle maximum corresponds to stationary thermomagnetic rolls.

Table 1: The critical values of $\widetilde{Gr}_m$, $\widetilde{Gr}$, $\tilde{\alpha}$, disturbance wave speed $\tilde{c} = -\tilde{\alpha}^I/\tilde{\alpha}$ and the maximum speed of the basic flow $\tilde{v}_{0\max}$ for mixed convection in a normal $(\delta = 0^o)$ magnetic field $H^e = 100$ at $\tilde{\chi} = \tilde{\chi}_* = 5$ and various values of Prandtl number $\widetilde{\Pr}$.

$\widetilde{\Pr}$	$\widetilde{Gr}_{mc}$	$\widetilde{Gr}_c$	$\tilde{\alpha}_c$	$\tilde{c}_c$	$\tilde{v}_{0\,max}$
20	0	150.864	0.821	±9.291	9.673
55	0	65.335	1.127	±4.203	4.189
70	0	56.780	1.164	±3.678	3.641
130	0	40.974	1.238	±2.692	2.627
20	9.087	0	1.937	0	0
55	3.305	0	1.937	0	0
70	2.596	0	1.937	0	0
130	1.398	0	1.937	0	0
20	12	148.721	0.829	±9.147	9.536
55	12	59.273	1.196	±3.785	3.800
70	12	49.547	1.260	±3.179	3.177
130	12	29.222	1.452	±1.881	1.874
55	30	45.380	1.365	±2.835	2.910

It is also observed that the basic flow becomes less stable when Prandtl number increases. Prandtl number is the ratio of fluids viscosity and thermal diffusivity. The large Prandtl number corresponds to small thermal diffusion and the thermal disturbances dissipate slowly in large Prandtl-number fluids (see Table 1). Therefore, we conclude that the physical natures of instabilities are thermal and because of that the waves are called thermal waves. Thermal waves propagate upward near the hot wall and downward near the cold wall. The representative critical values of $\widetilde{Gr}, \tilde{\alpha}$ and disturbance wave speed $\tilde{c}$ for two waves of mixed thermo-gravitational or magnetic convection in a normal magnetic field at $\widetilde{Gr}_{mc} = 12$ and $\widetilde{\Pr} = 55$ are given in Table 2 for various values of magnetic susceptibilities $\tilde{\chi}$ and $\tilde{\chi}_*$ In the case of linear magnetization law i.e., when $\tilde{\chi} = \tilde{\chi}_*$ the two waves propagate with equal speeds in the opposite directions.

Table 2: The critical values of $\widetilde{Gr}$, $\tilde{\alpha}$ and disturbance wave speed $\tilde{c} = -\tilde{\alpha}^I/\tilde{\alpha}$ for leading two waves of mixed convection in a perpendicular external magnetic field at $\widetilde{Gr}_{mc} = 12$, $H^e = 100$, $\widetilde{\Pr} = 55$ and various values of $\tilde{\chi}$ and $\tilde{\chi}_*$.

		$\delta = 0^o$					
		Upward wave			Downward wave		
$\tilde{\chi}$	$\tilde{\chi}_*$	$\tilde{\alpha}_c$	$\widetilde{Gr}_c$	$\tilde{c}_c$	$\tilde{\alpha}_c$	$\widetilde{Gr}_c$	$\tilde{c}_c$
5	5	1.196	59.28	3.785	1.196	59.28	-3.785
3	5	1.204	59.52	3.795	1.199	60.27	-3.845
3	3	1.198	58.86	3.758	1.198	58.86	-3.758
1.5	2.5	1.207	58.18	3.708	1.202	58.84	-3.752
1	2	1.207	58.32	3.716	1.200	59.38	-3.786
0.5	1.5	1.202	59.50	3.790	1.193	61.53	-3.923

However, when the values of $\tilde{\chi}$ and $\tilde{\chi}_*$ differ i.e., in the case of non-linear magnetization law closer to magnetic saturation, the symmetry of waves propagation is broken, and the upward wave near the hot wall becomes more dangerous compared to the downward wave near the cold wall (see Table 2).

6. REPRESENTATIVE STABILITY CHARACTERISTICS OF FLOWS IN OBLIQUE MAGNETIC FIELDS

The critical parameter values as functions of the magnetic field inclination angles are shown in figure 6. The flow is stable in the regions below the respective curves meaning that flow becomes more stable at larger field inclination angles. With the increase of field inclination angle _ the wavelength increases (see figure 6(b)) and as a result the distance between the rolls decreases. It follows from figure 6(c) that as the field inclination angle increases the wave speed also increases. The comparison of the critical parameter values for two waves at a fixed magnetic Grashof number fGrmc = 12 is shown in figure 7. The upward wave

is always characterized by a larger wave number compared to that of the downward wave as seen from figure 7(b) and, consequently, the corresponding instability rolls remain closer to each other compared to the downward wave.

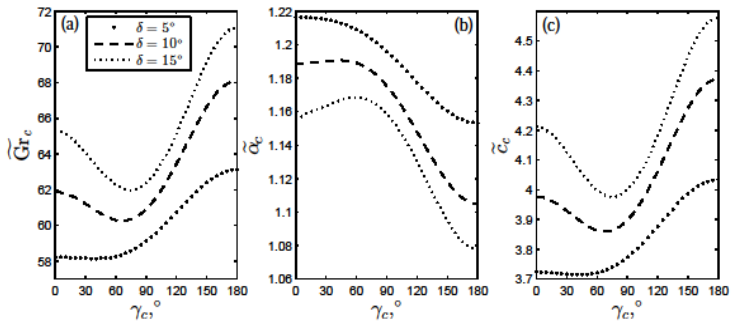

Figure 6: Comparison among the critical values: (a) Grashof number $\widetilde{Gr}_c$, (b) wave number $\widetilde{\alpha}_c$ and (c) wave speeds $\widetilde{c}_c$ as functions of the field inclination angle δ for $\widetilde{Gr}_{mc}=12, H^e=100, \widetilde{\mathrm{Pr}}=55, \widetilde{\chi}=1.5$ and $\widetilde{\chi}_*=2.5$.

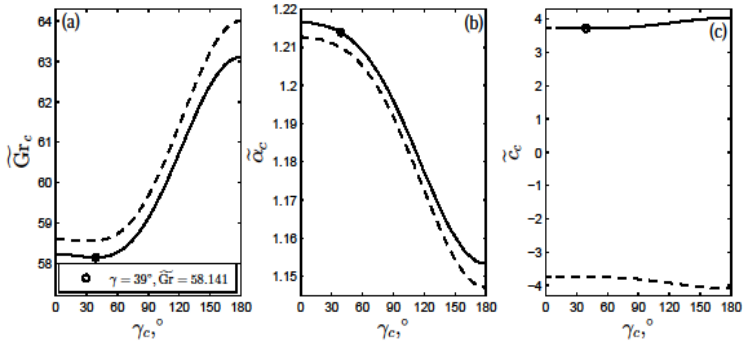

Figure 7: Comparison of the critical values for the first (solid line) and second (dashed line) wave modes: The flow is stable under the respective curve. (a) Grashof number $\widetilde{Gr}_c$, (b) wave number $\widetilde{\alpha}_c$ and (c) wave speeds $\widetilde{c}_c$ as functions of the azimuthal angle γ for $\widetilde{Gr}_{mc}=12, H^e=100, \widetilde{\mathrm{Pr}}=55, \widetilde{\chi}=1.5$ and $\widetilde{\chi}_*=2.5$.

The critical values similar to those given in Table 2 for the two counter-propagating waves in a mixed convection regime in various oblique magnetic fields are presented in Tables 3 and 4. In contrast to the normal field, the oblique magnetic field leads to the asymmetry in wave propagation regardless of whether the fluid magnetization is linear or non-linear in the flow domain.

Table 3: The critical values of $\widetilde{Gr}$, $\widetilde{\alpha}$ and disturbance wave speed $\widetilde{c}=-\widetilde{\alpha}^I/\widetilde{\alpha}$ for the upward wave of mixed convection in an oblique external magnetic field at $\widetilde{Gr}_{mc}=12$, $\gamma=0^o$, $\widetilde{\mathrm{Pr}}=55$, $H^e=100$ (odd-numbered lines) $H^e=10$ (even-numbered lines) and various values of $\widetilde{\chi}$ and $\widetilde{\chi}_*$

		$\delta=5°$			$\delta=10°$			$\delta=15°$		
$\widetilde{\chi}$	$\widetilde{\chi}_*$	$\widetilde{\alpha}_c$	$\widetilde{\mathrm{Gr}}_c$	$\widetilde{c}_c$	$\widetilde{\alpha}_c$	$\widetilde{\mathrm{Gr}}_c$	$\widetilde{c}_c$	$\widetilde{\alpha}_c$	$\widetilde{\mathrm{Gr}}_c$	$\widetilde{c}_c$
5	5	1.196	60.69	3.893	1.156	65.54	4.225	1.127	68.74	4.442
		1.205	60.08	3.853	1.163	65.01	4.190	1.131	68.45	4.422
3	5	1.196	62.15	3.992	1.147	67.93	4.386	1.118	70.78	4.579
		1.206	61.62	3.957	1.151	67.70	4.370	1.119	70.74	4.576
3	3	1.207	58.91	3.770	1.183	62.04	3.987	1.155	65.27	4.207
		1.212	58.59	3.749	1.190	61.59	3.957	1.160	64.91	4.183
1.5	2.5	1.217	58.22	3.723	1.189	61.85	3.974	1.159	65.28	4.209
		1.220	57.97	3.706	1.194	61.51	3.952	1.162	65.06	4.194
1	2	1.220	57.93	3.702	1.198	61.01	3.917	1.169	64.34	4.145
		1.222	57.76	3.690	1.202	60.74	3.899	1.172	64.16	4.133
0.5	1.5	1.220	58.37	3.729	1.206	60.80	3.903	1.180	63.96	4.120
		1.222	58.29	3.723	1.210	60.67	3.893	1.183	63.90	4.116

Tables 3 and 4 also confirm that the upward wave in various oblique magnetic fields is always characterized by a larger wave number than that of downward wave and this is consistent with numerical results presented in figures 6 and 7. Note from equation (14) that the magnitude of the non-dimensional magnetic field is proportional to parameter N, which is inversely proportional to the pyromagnetic coefficient that characterizes fluid magnetization, and thus the large value of non-dimensional magnetic field corresponds to weaker fluid magnetization and vice versa. Perturbation patterns in a stronger magnetized fluid in oblique magnetic field are characterized by larger wave numbers and ba- sic flow is less stable there than in a weaker magnetized fluid. The upward propagating wave remains the most dangerous as follows from corresponding data presented in Tables 3 and 4 (compare data for He = 100 in even-numbered and He = 10 in odd-numbered lines).

Table 4: Characteristics of the downward wave for the same vales as Table 3

		$\delta = 5^\circ$			$\delta = 10^\circ$			$\delta = 15^\circ$		
$\tilde{\chi}$	$\tilde{\chi}_*$	$\tilde{\alpha}_c$	$\widetilde{\mathrm{Gr}}_c$	$\tilde{c}_c$	$\tilde{\alpha}_c$	$\widetilde{\mathrm{Gr}}_c$	$\tilde{c}_c$	$\tilde{\alpha}_c$	$\widetilde{\mathrm{Gr}}_c$	$\tilde{c}_c$
5	5	1.194	60.86	-3.904	1.154	65.67	-4.233	1.126	68.81	-4.446
		1.181	61.80	-3.966	1.145	66.30	-4.275	1.122	69.11	-4.466
3	5	1.194	61.97	-3.985	1.147	67.35	-4.355	1.118	70.22	-4.548
		1.182	62.65	-4.032	1.142	67.56	-4.369	1.117	70.25	-4.551
3	3	1.206	58.99	-3.775	1.182	62.15	-3.994	1.154	65.35	-4.213
		1.200	59.44	-3.805	1.174	62.72	-4.032	1.148	65.75	-4.240
1.5	2.5	1.212	58.62	-3.751	1.186	62.00	-3.988	1.156	65.29	-4.213
		1.208	58.95	-3.773	1.179	62.40	-4.014	1.152	65.53	-4.229
1	2	1.214	58.54	-3.744	1.193	61.21	-3.935	1.166	64.30	-4.148
		1.211	58.73	-3.758	1.188	61.50	-3.955	1.162	64.49	-4.160
0.5	1.5	1.213	59.51	-3.808	1.200	61.07	-3.928	1.177	63.64	-4.110
		1.211	59.53	-3.810	1.196	61.15	-3.935	1.174	63.66	-4.112

7. COMPLETE STABILITY DIAGRAMS FOR AN EQUIVALENT TWO-DIMENSIONAL PROBLEM

To identify parametric regions where different physical mechanisms lead to the onset of instability in the considered geometry, the complete stability diagrams for an equivalent two dimensional problem are computed. The stability diagram for normal magnetic field and Prandtl number Pr = 55 is shown in figure 8.

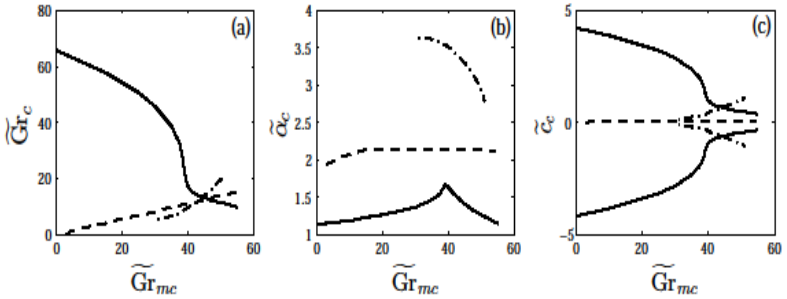

Figure 8: (a) Stability diagram for an equivalent two-dimensional problem; (b) critical wave number $\tilde{\alpha}_c$ and (c) the corresponding wave speed $\tilde{c}_c$ along the stability boundaries shown in the plot (a) for $\widetilde{\mathrm{Pr}} = 55, \delta = \gamma = 0^o$ and $\chi = \tilde{\chi}_* = 5$.

It consists of three lines each representing different type of instability characterized by its own wave number as follows from figure 8(b). The solid line in figure 8(a) starts from $\widetilde{Gr}_{mc} = 0$, which corresponds to the threshold of classical thermo-gravitational convection instability. As discussed earlier this type of convection is characterized by two counter-propagating thermal waves investigated in [8, 9, 10, 2]. However, along the solid line the role of magnetic effects increases at the expense of thermal effects so that thermo-gravitational instability is gradually replaced with the thermomagnetic one. The basic flow is stable in the region below the solid line. The dashed line in figure 8(a) starts from $\widetilde{Gr}_c = 0$ and therefore corresponds to the threshold of magneto-convection. In this case, the disturbance amplification rate $\tilde{\sigma}^R$ is real (see figure 4). As follows from an earlier discussion this type of instability is characterized by a stationary pattern and this is consistent with the previous investigations [7, 11]. The basic flow is stable above the dashed line. The dash-dotted line corresponds to the thermo-gravitational/thermomagnetic convection instability. The basic flow is stable below it. As seen from figure 8(b), thermo-gravitational convection patterns have smaller wave-numbers (the solid line) than those of stationary magneto-convection (the

dashed line). The stationary magneto-convection patterns also have smaller wave-numbers than those of mixed magneto-gravitational convection (the dash-dotted line). The wave speed of the disturbance thermal waves corresponding to the thermo-gravitational convection instability is larger than that of the mixed magneto-gravitational convection instability (compare the solid & dashdotted lines in figure 8(c)). The disturbance thermal wave speed also decreases when magnetic effects become stronger (compare wave speeds for two sets of data $(\tilde{G}r_{mc} = 12, \tilde{G}r_{mc} = 59.273)$, $(\tilde{G}r_{mc} = 30, \tilde{G}r_{mc} = 45.38)$ presented in Table 1). The mixed magneto-gravitational convection is characterized by two counter-propagating thermomagnetic waves with smaller wave speed (right ends of the solid and dash-dotted lines in figure 8(c)). The pure magneto-convection is characterized by a stationary pattern as the corresponding values $\tilde{c}_c = \tilde{\sigma}^I = 0$ (the dashed line in figure 8(c)).

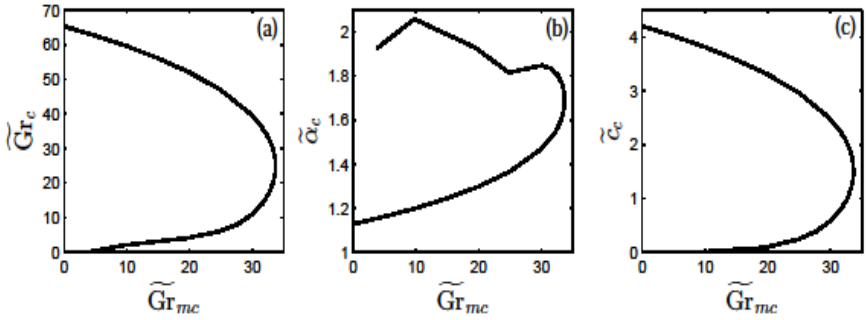

Figure 9: Same as Figure 8 but for $\delta = 5^o$ and $\gamma = 0^o$

The stability diagram for oblique magnetic field $\delta = 5^o, \gamma = 0^o$ shown in figure 9 is computed using the same parameter values as in figure 8. It is remarkable that the qualitative change in stability diagram occurs even for such small field inclination angles. The solid and dashed stability boundary lines distinguished in figure 8(a) merge in figure 9(a). The dash-dotted line in the lower right corner in figure 9(a) almost completely disappears. As follows from figure 9(a) even though the solid line originates from fGrc = 0 it corresponds to non-stationary magnetoconvection as the corresponding eigen-values shown in figure 10 have non-zero imaginary parts.

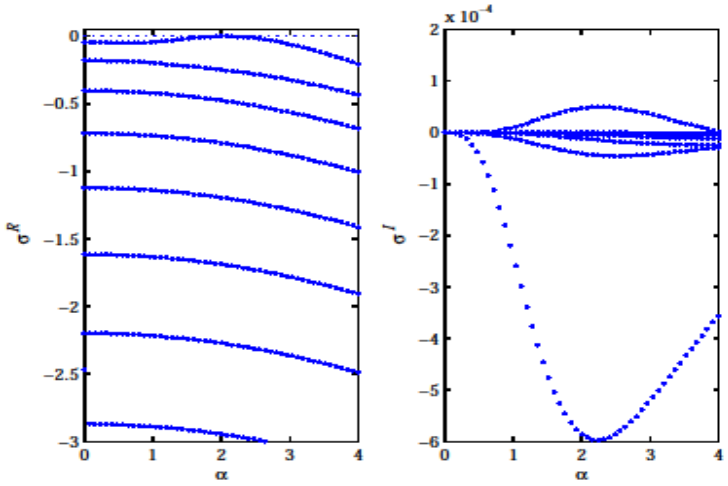

Figure 10: Same as Figure 3 but for $(\tilde{G}r_m, \tilde{G}r) \equiv (6.04, 0)$ and $\delta = 5^o, \gamma = 0^o$.

The flow stability region becomes larger in an oblique magnetic field (compare the stability regions in figures 8(a) and 9(a)) and this is consistent with the numerical results given in Tables 2, 3 and 4. As follows from figure 9(b), the thermomagnetic convection instability is characterized by a smaller wave number (the solid line) compared to that of the mixed magneto-gravitational convection (the dash-dotted line). As discussed earlier, regardless of whether the magnetization law is linear or not the symmetry of the disturbance thermal waves propagation is broken in oblique field and the upward wave becomes more dangerous. Therefore, in figure 9(c) only the critical wave speed for this wave is shown. It increases monotonically with $\tilde{G}r_c$.

8. CONCLUSIONS

The linear stability of thermomagnetic-gravitational convection has been investigated in the same geometry as pure thermomagnetic convection. In this case, it is noticed that two distinct mechanisms, thermo-gravitational and thermomagnetic acting simultaneously, are responsible for the appearance of various instability modes. Thermomagnetic convection is happen by the spatial variation of the fluid magnetization and magnetic field across the non-uniformly heated layer. The characteristics of all instability modes are investigated as functions of the inclination and orientation angles and the magnitude of the applied magnetic field for various values of magnetic parameters and for linear and non-linear magnetization laws when both the thermomagnetic and buoyancy mechanisms are active. Three main types of instability patterns corresponding to thermo-gravitational, magnetic and magneto-gravitational convection are found to exist. In a normal magnetic field the stability characteristics of the flow are independent of the magnitude of the applied normal magnetic field. The inclination of the external magnetic field leads to the preferential shift of instability structures toward the hot wall, which is more pronounced in magnetically more sensitive fluid characterized by a smaller non-dimensional magnetic field magnitude. It is demonstrated that in magneto-gravitational instability regime two waves propagate inside the layer: up near the hot wall and down near the cold one. The upward propagating wave becomes more dangerous in all regimes regardless of whether the fluid magnetization law is linear or not. The comparison of the up- and downward propagating waves shows that the upward propagating wave is characterized by a lager critical wave number compared to that of the downward one. The basic flow becomes more stable and the disturbance waves propagate quicker while the field inclination angle increases. The stability characteristics of the basic flow regarding the wave-like disturbances have been compared for thermo-magnetically less and more sensitive fluids, and it has been observed that the upward propagating wave remains the most dangerous in both types of fluids.

REFERENCES

[1] S. Odenbach, “Ferrofluids: magnetically controllable fluids and their applications,” Springer, New York, 2002.

[2] S. A. Suslov. “Thermo-magnetic convection in a vertical layer of ferromagnetic fluid,” Phys.Fluids, 20(8):084101, 2008.

[3] S. A. Suslov, A. A. Bozhko, A. S. Sidorov, and G. F. Putin, “Thermomagnetic convective flows in a vertical layer of ferrofluid: Perturbation energy analysis and experimental,” Phys. Rev. E, 86:016301, 2012.

[4] H. Rahman and S. A. Suslov. “Thermomagnetic convection in a layer of ferrofluid placed in a uniform oblique external magnetic fluid,” J. Fluid Mech., 764:316–348, 2015

[5] H. Rahman and S. A. Suslov, “Magneto-gravitational convection in a vertical layer offerrofluid in a uniform oblique magnetic field,” J. Fluid Mech., 795:847-875, 2016.

[6] S. A. Suslov, A. A. Bozhko, and G. F. Putin, “Thermo-magneto-convective instabilities in a vertical layer of ferro-magnetic fluid,” In Proceedings of the XXXVI International Summer School—Conference “Advanced Problems in Mechanics”, pages 644–651, Repino, Russia, 2008

[7] B. A. Finlayson, “Convective instability of ferromagnetic fluids,” J. Fluid Mech., 40:753–767, 1970.

[8] G. Z. Gershuni, E. M. Zhukhovitsky, and A. A. Nepomniaschy, “Stability of Convective Flows,” Science, Moscow, Russia (in Russian), 1989

[9] A. Chait and S. A. Korpela, “The secondary flow and its stability for natural convection in a tall vertical enclosure,” J. Fluid Mech., 200:189–216, 1989.

[10] S. Wakitani, “Formation of cells in natural convection in a vertical slot at large Prandtl number,” J. Fluid Mech., 314:299–314, 1996.

[11] B. L. Smorodin, M. Shliomis, and P. Kaloni, “Influence of a horizontal magnetic field on free ferrofluid convection in a vertical slot,” Book of abstracts, 11 International conference on Magnetic Fluids, Kosice, Slovakia, pages 6–22, July 23–27, 2007.

[12] J. Huang, B. F. Edwards, and D. D. Gray, “Thermoconvective instability of paramagnetic fluids in a uniform magnetic field,” Phys. Fluids, 9(6):1819–1825, 1997.

[13] A. F. Pshenichnikov, “A mutual-inductance bridge for analysis of magnetic fluids,” Instrum. Exp. Tech., 50(4):509–514, 2007.

[14] A. V. Lebedev and S. N. Lysenko, “Magnetic fluids stabilized by polypropylene glycol,” J. Magn. Magn. Mater., 323:1198–1202, 2011